2010 IEEE/ASME International Conference on
Advanced Intelligent Mechatronics
Montréal, Canada, July 6-9, 2010

Design and development of a low-cost interferometric device for nanoscale position and velocity feedback

Dimitrios Felekis and Evangelos Papadopoulos, *Senior Member, IEEE*

***Abstract*— A low-cost interferometer for piezoelectric actuator (PEA) displacement and velocity feedback was developed and described here. An initial design employed a single photodiode as a sensing element. Although fringes could be measured successfully, to obtain the direction of displacement, the PEA control input was needed. A low-cost interferometric encoder is developed that employs a pair of silicon photodiodes and a manual micropositioner stage. With this system, the actuator input is not needed for direction determination, while a 158.2 nm resolution is achieved. Algorithms for the single photodiode and for the interferometric encoder were developed and are described in detail. The results were verified using a PEA-embedded strain gage. The developed device can be used for PEA characterization and for real-time position and velocity control of micromechanisms and microrobots.**

***Index terms*– Michelson interferometer, fringe counting, nanoscale position feedback, piezoelectric actuators.**

I. Introduction

A difficult task in microsystem technology is the measurement of microactuator or micromechanism displacements and velocities, without influencing the measured variable. This task becomes important during piezoelectric actuator characterization, or during position control of microrobots at sub-micron accuracy.

Candidate contact sensors for such measurements include strain gauges, capacitive sensors and LVDTs. Strain gauges are widely used in the indirect metrology of piezoelectric actuator (PEA) displacements. Although their resolution is high, they demand very careful mounting. In addition, they cannot be used in measuring displacements of mobile microrobotic systems. Capacitive sensors yield nanometric resolution, and excellent linearity, but their size and mass has an adverse effect on the inertia of the system to be measured, and therefore on the measurement itself. Another candidate sensor is the LVDT. These sensors have high resolution, but are subject to friction between the coil and the core, with the latter being attached on the system under measurement. In addition, the mass of the core is often greater than that of the element whose displacement must be measured, and as a result the results are corrupted.

Non-contact measurement methods have obvious advantages compared to contact ones, as they do not affect the measured variable. The prime non-contact method is that of interferometry, with the Michelson interferometer being an obvious candidate measurement system. This kind of optical sensor is used for the measurement of displacements with micrometer or even nanometer accuracy. Several papers have been published, where the task is to measure displacements, [1-4]. If both the measurement of the displacement and the identification of its direction are needed, a Fabry-Perot type interferometer is used, [5]. Efforts have been made in using a laser diode as a source in interferometers aiming at a reduced total cost, [6, 7].

We looked at the above technologies, as we were interested in identifying the parameters of piezoelectric actuators and to develop sensor techniques for microrobots. Interferometry appeared more interesting due to the reasons discussed above. The flexible design of interferometers satisfies specifications such as size and low budget. Also, these devices offer the possibility for two-axes measurements, as well as for measuring displacements of other micro-systems without affecting the functionality of the device. However, we were interested in obtaining not only displacements, but also direction of motion and velocities in a form that can be used in real-time closed-loop control, as required in the control of the microrobots developed at the NTUA Control Systems Laboratory, [8].

In this paper, we present the development of a low-cost interferometer employing a novel interferometric encoder. Although Michelson interferometry is a well-known method for displacement measurement, it has not been used in servo-control due to the lack of a direction sensing functionality. First, basic interferometer theory elements are discussed. Here, a typical Michelson interferometer with a slightly tilted fixed mirror is used in order to produce vertical and equally spaced fringes. The interferometer was developed and built from readily available hardware and its structure is presented in detail. A relatively simple and fast algorithm developed for fringe counting and direction of motion detection is described. With this device, one is able to measure displacements by fringe counting and to identify the direction of motion using a pair of photodiodes and the developed algorithm. Experimental results and algorithms are given that demonstrate the benefits of the design.

II. Theory & Analysis

In this work, a custom low-cost Michelson interferometer is proposed for the measurement of displacements and

Dimitrios Felekis was with the Department of Mechanical Engineering, National Technical University of Athens, Greece. He is now with the ETH, Zurich, Switzerland (e-mail: dfelekis@ethz.ch).

Evangelos Papadopoulos is with the Department of Mechanical Engineering, National Technical University of Athens, Greece (phone: +30-210-772-1440; fax: +30-210-772-1450; e-mail: egpapado@central .ntua.gr).

velocities of PEAs by counting the fringes produced. Fig. 1 shows the interferometer principle of operation. A laser beam starting at S is split in two. One beam is reflected at the beam splitter and follows the R, R’ path to the screen, after a reflection at the fixed mirror M_2. The other beam passes through the splitter and follows the T, T’ path, after a reflection at the moveable mirror M_1. The fixed mirror is tilted slightly in order to produce equally spaced fringes on the screen of the interferometer. A displacement of the moveable mirror M_1, caused by a PEA attached to it, changes the length of the optical path and thus the fringe pattern obtained at the screen.

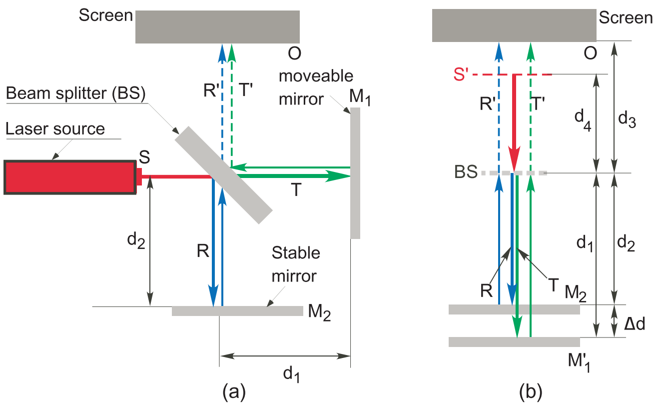

Fig. 1. (a) Michelson interferometer schematic representation, and (b) linear equivalent representation.

Using the motion of the fringes, we calculate the overall displacement of the moveable mirror, and as a consequence the displacement of the PEA that caused the mirror to move. In Fig. 1b, the linear equivalent of the Michelson interferometer of Fig. 1a is depicted. The blue line represents the beam R reflected on the beam splitter, whereas the green line is the transmitted beam T. M_1 is the moveable mirror, M_1' is its linear equivalent, and d_1 is its distance from the beam splitter. Also, d_2 is the distance of the fixed mirror from the beam splitter and d_3 is the distance of the beam splitter to the screen. The distance of the beam splitter from the linear equivalent of the laser source S’, is d_4. According to Fig. 1b, the two optical paths equal to,

$$\begin{aligned} r_1 &= 2d_1 + d_3 + d_4 \\ r_2 &= 2d_2 + d_3 + d_4 \end{aligned} \tag{1}$$

The intensity of linearly polarized waves of equal amplitude E_0 is given by,

$$E_i = E_0 \cos(k \cdot r_i - \omega t + \varepsilon_i) \tag{2}$$

where k is the propagation number, r_i is the optical path length to the screen, ε is the initial phase or epoch angle, ω is the angular frequency, and i = 1, 2 for the two beams [9-13]. The irradiance at a point on the screen is given by,

$$I = \varepsilon_0 c \langle \mathrm{E}^2 \rangle \tag{3}$$

where $\langle \mathrm{E}^2 \rangle$ indicates the time average of the magnitude of the electric field intensity, and ε_0 and c are the permittivity and the speed of light in the vacuum respectively. Since we are concerned with relative irradiances within the same medium, we neglect the constants and set,

$$I = \langle \mathrm{E}^2 \rangle \tag{4}$$

In our case, the amplitudes of both waves are equal which means that the irradiance contributions from both sources are equal. Additionally, the two waves are from the same emitter and thus they are in phase. Then, the intensity at a given point is given by,

$$I = 2I_0(1+\cos\delta) = 4I_0 \cos^2 \frac{\delta}{2} \tag{5}$$

where δ is the phase difference from a combined path-length and epoch-angle difference. According to Fig. 1, δ equals to,

$$\delta = k(r_1 - r_2) = k(d_1 - d_2) = k \cdot 2\Delta d \tag{6}$$

In order for the irradiance to become maximum, corresponding to a light fringe, the term δ has to be an integer multiple of the wavelength. That is,

$$\delta = 2\pi m \;\Leftrightarrow\; 2\Delta d_l = \lambda m \tag{7}$$

Respectively, minimum irradiance, which corresponds to a dark fringe, occurs when

$$\delta = \pi(2m+1) \;\Leftrightarrow\; 2\Delta d_d = \lambda\left(m + 1/2\right) \tag{8}$$

Subtracting (7) from (8), we find the difference between a dark fringe and the adjacent light fringe in terms of displacement of the moveable mirror,

$$2\Delta d_{l,d} = \frac{\lambda}{2} \Leftrightarrow \Delta d_{l,d} = \frac{\lambda}{4} \tag{9}$$

The meaning of the above equation is that the moveable mirror has to be moved by λ/4 in order for a dark fringe to take the place of the adjacent light fringe and vice versa. Thus, the total displacement can be derived from the number of fringes crossing a specific point on the screen by,

$$d = \mathrm{N} \cdot \frac{\lambda}{4} \tag{10}$$

where N is the number of changes between dark and light fringes at a specific point on the screen, and λ is the wavelength of the light source used. For the He-Ne laser used in our case, λ = 632.8 nm, and therefore, the resolution achieved is 158.2 nanometers.

III. Experimental Setup

A. *Experimental Approach*

For the PEA displacement measurement, three alternative methods were used. First, a custom Michelson interferometer with one silicon photodiode as a photosensor was developed. However, for the fringe counting algorithm to work properly, the direction of PEA motion must be known, which can be obtained by the input voltage to the PEA. However, the algorithm becomes more complicated, time consuming and hard to apply.

To overcome this problem, a novel interferometric encoder was developed. This device works as a photosensor on the interferometer screen and additionally allows estimation of the instantaneous PEA direction of motion. Consequently, the fringe counting algorithm becomes simpler and faster. Finally, to verify the experimental results, we used strain gauges to measure PEA displacement.

Fig. 2 shows the flow chart of the experimental procedure followed. First, a voltage signal is generated from Agilent 33220A waveform generator which is then amplified in the Piezomechanik LE 150/25 PZT amplifier and finally an offset is added to achieve a voltage range from 0V to +150V. The amplified voltage serves as the input to the actuator that is placed on behind the moveable mirror. By changing the deflection of the actuator, the optical path as well as the fringes that are produced on the screen change. As a result, the light intensity on the photodiode changes and produces a current flow that is converted to voltage by an I-V converter circuit [14,15]. Finally, this voltage signal is acquired by the National Instruments PCI 6036E DAQ Card and is processed on a PC.

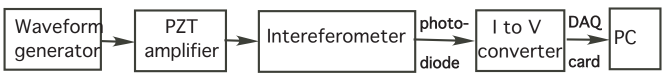

Fig. 2. Flow chart of the experimental procedure.

B. *Custom Michelson Interferometer*

The custom interferometer developed includes the following main parts, (a) a laser source, (b) a beam splitter, (c) a fixed mirror, and (d) a moving mirror, see Fig. 3. The laser source used is a JDSU He-Ne laser of 632.8 nm wavelength, 5-10 mW output power range and 0.81mm beam diameter. The laser is of higher power than needed here to allow us measure displacements in more than one axes in the future.

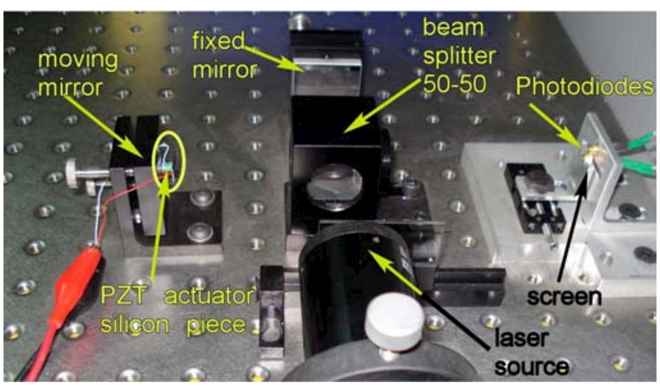

Fig. 3. Custom Michelson interferometer setup.

The beam splitter has a 50/ 50 reflection-transmission ratio and is of cubic type for higher stability. Its housing has four threaded apertures. On the aperture facing the screen, a biconcave lens is attached to allow for spreading the interference fringes. The fixed mirror is attached on a 1.50'' steel mirror mount. Its surface is of ¼ wavelength accuracy, at 632.8 nm. Two fine resolution adjustment screws allow precise tilting of the mounting surface in two directions.

Aiming at measuring the deflection of the PEA actuator we have replaced the moving mirror by a system of actuator-silicon wafer. The silicon wafer serves as a reflective surface (mirror) and is attached on the front end of the actuator. Hence, by changing the actuator displacement through its input voltage, we change the optical path length resulting in a fringe pattern change.

In Fig. 4, the PEA ramp input voltage and the corresponding raw signal from a single photodiode is shown for three ramps. As the actuator moves, the fringe pattern changes and the photodiode signal changes accordingly from maximum, i.e. light fringe, to minimum, i.e. dark fringe.

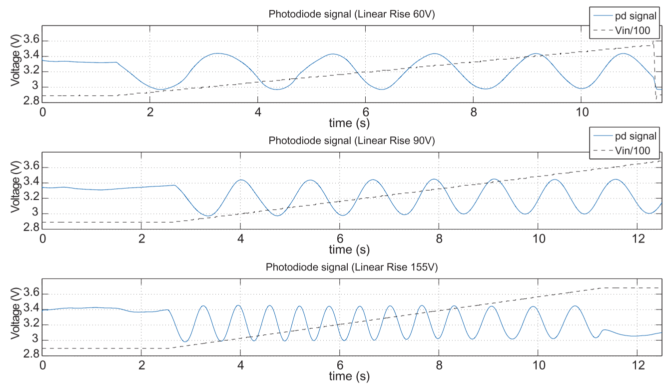

Fig. 4. Photodiode signal output for three ramp input voltages with increasing voltage amplitude at the same frequency.

C. *Interferometric Encoder*

The sensing part of the setup is based on a silicon photodiode. This sensor was chosen since it satisfies our requirements, i.e. small size, active area that covers the laser beam diameter, good linearity between light intensity (input) and current output, and low cost.

To know the direction of PEA motion, one photodiode is not enough, as it cannot discriminate between pulses of either direction. To this end, a novel interferometric encoder using two photodiodes and based on the concept of the optical encoder was developed. A CAD representation of the encoder and its parts is shown in Fig. 5(a).

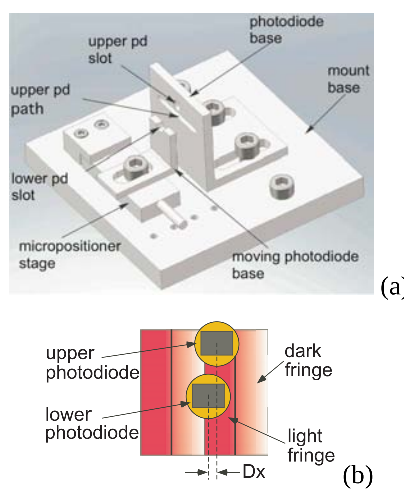

Fig. 5. (a) CAD representation of the interferometric encoder, and (b) photodiode placement for achieving out of phase signals.

Direction sensing, with the interferometric encoder, requires that the signals from two photodiodes be out of phase with respect to each other by 90^o. To achieve this, one must manually create a Dx, see Fig. 5(b), that is a multiple of the distance from the centre of a light fringe to the centre of the adjacent dark fringe plus ¼ times this distance. To this end, the lower photodiode is mounted on a base connected through an angle bracket to a linear micropositioner with micrometric resolution. This serves to change the lower photodiode's position relatively to the upper photodiode's position and therefore achieve the required offset of the two.

IV. Algorithm For Fringe Counting

As described above, to convert the fringe motion to displacement, we need to trace the extrema of the photodiode waveform. Finding the extrema of the photodiode signal was challenging due to the optical and electrical noise in the signal. Efforts included the use of routines from the LabVIEW environment and signal derivation but with no success due to noise. To avoid the noise related problems, we chose first to convert the signal to pulses and then to work on the fringe counting. For the conversion of the waveform to pulses, we used a Schmitt trigger approach. According to this method, the pulse values are one or zero. The user inputs an upper and a lower threshold. When the value of the signal exceeds the upper threshold, the pulse becomes one and holds this value until the signal drops under the lower threshold and the pulse becomes zero. Also, the zero value remains until the waveform exceeds the upper threshold.

In the first series of experiments conducted, the setup with one photodiode was used. A difficulty that arises with this method is the lack of information on the points where the actuator direction is changed. To overcome this problem, we used the PEA input signal to get a first estimate of the data series range in which a change in direction occurs, and then we scan the series in this range to find the exact point of direction change. This is not enough, as we also need to know if a backward or forward displacement occurs. This information also can be extracted from the PEA input signal. Although the algorithm built based on the above can work, it tends to be complicated and computationally expensive. However, our intention was to design a flexible device that would allow us to measure displacements of different kinds of systems as well as to identify the direction of the moving system without the need of the PEA input signal. This led to the use of the two-photodiode interferometer and of an algorithm developed to extract information from the signals.

Fig. 6 shows the signals obtained from the two photodiodes during the motion of a mirror-bearing PEA. At the beginning of the experiment, the upper photodiode is at maximum intensity, i.e. on a light fringe, while the lower photodiode is at a centre-to-centre distance of ¼ times the distance between a light and a dark fringe. Observation shows that during a forward motion, the upper photodiode's signal is 90^o ahead, while during a backward motion, the lower photodiode's signal is 90^o ahead.

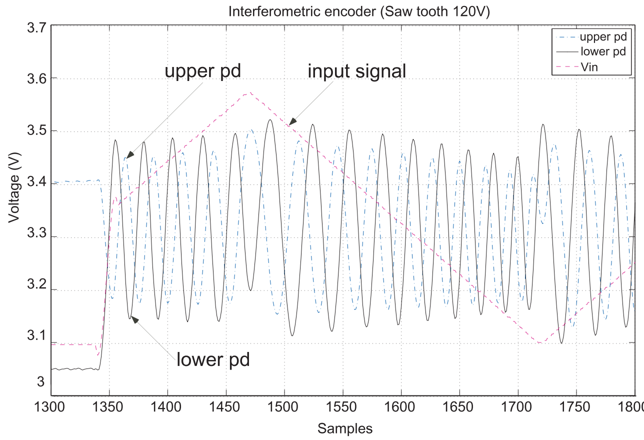

Fig. 6. Signals from the two photodiodes and the input voltage signal.

A. *Fringe Counting Algorithm*

The major steps of the algorithm developed are presented here. These include:

- Convert the photodiode signals to pulses with the Schmitt trigger method described above.
- Scan the entire experimental data set and determine the kind of motion that occurs. These are identified based on the following cases:
  1. Forward motion
     - (a) Transition of the upper photodiode from 1→0 and lower photodiode value 1, point A1 in Fig. 7.
     - (b) Transition of the upper photodiode from 0→1 and lower photodiode value 0, point A2 in Fig. 7.
  2. Backward motion
     - (a) Transition of the upper photodiode from 1→0 and lower photodiode value 0, point B1 in Fig. 7.
     - (b) Transition of the upper photodiode from 0→1 and lower photodiode value 1, point B2 in Fig. 7.
- Finally, the backward, forward and total displacements are calculated.

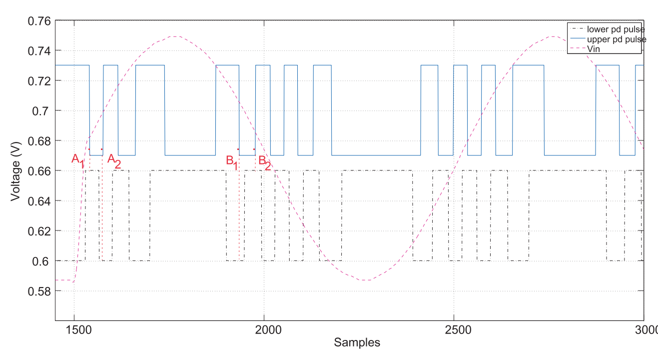

Fig. 7. Pulses created from photodiode signals and input signal.

From the fringe counting algorithm, we also get the timestamp of the occurrence of a step, as well as the contribution of this step to forward or backward motion. Thus, we can construct the waveform of actuator displacement that is required for calculating speed, acceleration and for study of nonlinear phenomena such as actuator hysteresis, creep, etc.

V. Experimental Results

Three different methods for measuring PEA displacements were used. The first used the Michelson interferometer with one photodiode. The second used the interferometer but with the two-photodiode interferometric encoder. The third method employed PEA-attached strain gages to verify the measurements obtained with the previous two methods.

Fig. 8 shows experimental results obtained from the single photodiode setup. Here we transform the signal to one and zero pulses as well. Firstly, the user defines an upper and lower threshold for the pulse conversion. When the value of the signal exceeds the upper threshold, point A in Fig. 8, the pulse becomes one and holds this value until the signal drops under the lower threshold, point B in Fig. 8, where the pulse becomes zero. Also, the zero value remains until the waveform exceeds the upper threshold. Having the pulse signal, we proceed to the calculation of displacement.

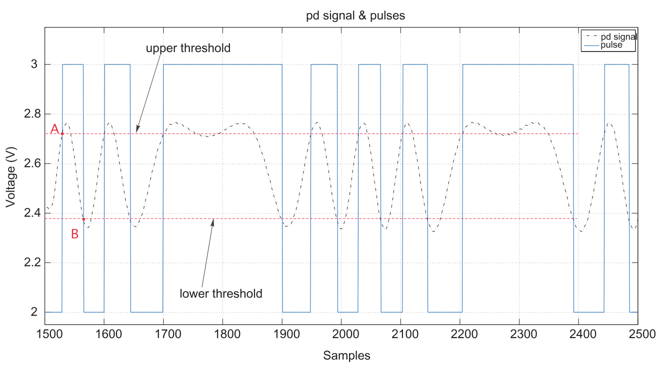

Fig. 8. Signal photodiode signal and generated pulses.

As we see in Fig. 8 the only information we can deduce from the data acquired is that of a displacement step when the change from a dark to a light fringe and vice versa takes place. To decide the direction of deflection, we acquire the input to the PEA voltage and compute its slope at the moment when the fringe change takes place. By doing so, we find if the PEA is moving forward or backwards.

This approach is very time consuming and requires sampling of the input to the moving system by appropriate hardware. Although this is possible for PEAs, this may not be the case with other systems.

An additional difficulty that arises with this method is the lack of information on the points where the actuator's direction is changed. Usually, when the direction changes, the transition from a light to a dark fringe and vice versa is not a full one. Thus, the signal value does not reach the upper or lower threshold, and as a result, the pulse value does not change. In this region we need to trace the exact points of the extremes in order to construct the displacement waveform. Again here we must use the input voltage to get the exact timestamp of change in direction.

The fringe counting algorithm for this method begins by creating the pulses from the photodiode signal. Then we track the points of maximum and minimum intensity (light and dark fringes) and their timestamps. Then, we check the vicinity of the input signal, for every timestamp found at the previous step, to identify a back or front motion. Finally, from (10) we calculate the total displacement of the PEA. It is clear that tracking the input signal adds to complexity and computation time, reducing the method's usefulness.

We next focus at the two-photodiode method and algorithm developed. In Fig. 9 the signal from both photodiodes and the input voltage signal is shown. For the sake of better display, the input voltage is scaled to appear at the same level as the photodiode signals. It is observed that a forward motion of the actuator causes a left fringe movement and a rear actuator movement causes a right fringe movement.

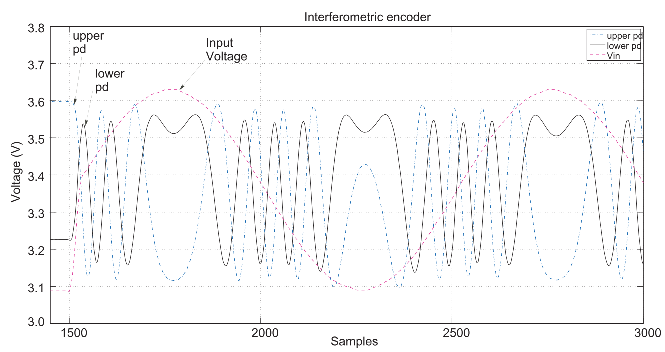

Fig. 9. Signals from both photodiodes and scaled input voltage signal.

To measure the displacement, the signal from the photodiodes is converted to pulses, as described above. The pulses that correspond to the experiment of Fig. 9 are shown in Fig. 7. The input signal is a 54V sinusoidal input but is scaled at the level of the pulses for better depiction. After having the pulses created, the whole data set is scanned and the net as well as the total displacement is calculated.

The next step is to create the displacement waveform from the photodiode's signal. In order to achieve this, the exact points of minima and maxima must be traced. Using the information from the both photodiodes we search for the signal extremes.

In Fig. 10, the intensity extremes are indicated by red circles. The displacement from one extreme to the adjacent one is λ/4 according to (10). However, we observe that when a change in direction occurs, as for example at points A and B in Fig. 10, the change from a dark to a light fringe and vice versa does not necessarily correspond to a minimum or a maximum in sensor reading.

Assuming that the fringes are of uniform illumination, we compute the exact displacement x by:

$$x = \frac{|V_B - V_A|}{V_{\max} - V_{\min}} \cdot \lambda/4 \qquad (11)$$

where V_A, V_B is the photodiode sensor output at points A and B and $V_{\min}, V_{\max}$, the minimum and maximum sensor reading, all converted in Volts.

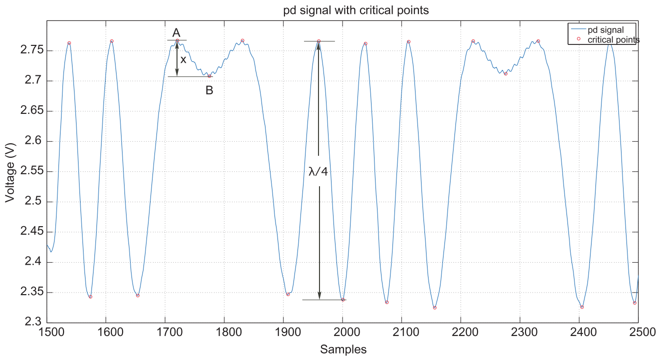

Fig. 10. Points of minimum and maximum light intensity.

Using the aforementioned method we obtain the displacement waveform shown in Fig. 11. It is easy now to use this waveform to compute the velocity of the actuator or to study of non-linear phenomena.

In order to verify the results obtained with the previous two methods, we conducted measurements with the same type of actuators but with strain gauges attached. The circuitry and all the software needed for this case were custom made. The strain gage was connected to a Wheatstone bridge and the signal was amplified in two stages and then filtered.

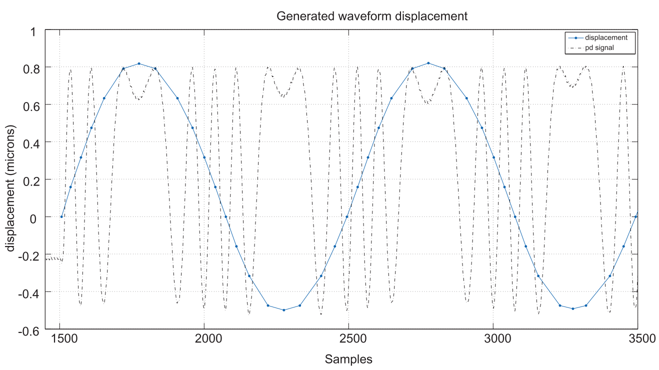

Fig. 11. Generated waveform of displacement for a sinusoidal input.

Table 1 shows the maximum deflection achieved for input voltages of 60, 120 and 150 Volts. We observe an error between the two methods of about 10%. The error presented may result from a small interferometer misalignment, noise introduced in the signal, not exact knowledge of the gain of the photodiodes or a miscalculated gain for the circuits used with the strain gage.

TABLE 1. RESULTS OF FRINGE COUNT ALGORITHM WITH INTERFEROMETRIC ENCODER AND STRAIN GAUGE

Input Voltage (V)	Deflection w. interferometer (μm)	Deflection w. strain gauge (μm)
60	1.58	1.68
120	3.00	3.24
150	3.96	4.10

It is worth noting that the complete fringe counting algorithm can be easily implemented in real-time running either on a PC with a real-time operating system or on an appropriate microcontroller.

VI. CONCLUSIONS & FUTURE WORK

The aim of the work described here was to develop a measuring system that could be used for position and velocity control of micromechanisms and systems performing movements with micrometer accuracy. To this end, a low-cost custom Michelson interferometer was developed to measure the displacement and direction of piezoelectric actuator motions. A novel interferometric encoder was designed and built that is used for direction sensing and displacement measurement with a resolution of 158.2 nm. The low-cost encoder uses two simple silicon photodiodes and a manual micropositioner stage. Algorithms for the fringe count in the case of the simple photodiode and the interferometric encoder method were developed. Measuring the displacement for the same input signals, using strain gages, validates the measurement results.

In the near future, we aim at identifying and eliminating the error sources. Furthermore, we work towards the application of the device to the position control of the microrobotic platform developed at CSL [8].

REFERENCES

[1] N. Bobroff, "Recent advances in displacement measuring interferometry," *Meas. Sci. Technol.*, vol. 4, pp. 907–926, Sept. 1993.

[2] J. Hoon, S. Hyun, Y. Kwak, "Peak movement detection method of an equally spaced fringe for precise position measurement," *Meas. Sci. Technol.*, vol. 41, pp. 428–434, Feb. 2002.

[3] J. Hoon, S. Hyun, Y. Kwak, "A nanometric displacement measurement method using the detection of fringe peak movement," *Opt. Eng.*, vol. 11, pp. 1352–1358, Sept. 2000.

[4] H. J. Martens, "Generalization and analysis of the fringe counting method for interferometric measurement of motion quantities," *Measurement.*, vol. 25, pp. 71-87, Jan. 1999.

[5] B. Neumann, U. Müller, "Fabry Perot interferometer with a quarter wave retarder and an intermediate exit for displacement measurements," *Optik-International Journal for Light and Electron Optics*, vol.112, pp. 81-85, Feb. 2001.

[6] S. Fletcher, A. Longstaff, A. Mayers, "Investigation into the accuracy of a proposed laser diode based multilateration machine tool calibration system," *J. Phys.: Conf. Ser*, vol.13, pp. 398-401, 2005.

[7] J. A. Stone, A. Stejskal, L. Howard, "Diode lasers in length metrology: Application to absolute distance interferometry," in *Proc. Meas. Sci. Conf.*, Anaheim, CA, 1999, pp. 1–7.

[8] P. Vartholomeos, "Modeling and Control of Microrobotic Systems," Ph.D. dissertation, Dept. Mech. Eng., National Technical Univ., Athens, GR, 2007.

[9] J. Dyson, *Interferometry as a measuring tool.* Brighton: The Machinery Publishing Co, 1970.

[10] P. Hariharan, *Optical Interferometry*. Sydney: Academic Press, 2003.

[11] P. Hariharan, *Basics of Interferometry*. Sydney: Academic Press, 1992.

[12] E. Hecht, A. Zajac, *Optics*. London: Addison-Wesley, 1974.

[13] S. Tolansky, *An Introduction to interferometry*. London: Longman, 1973.

[14] J. Graeme, *Photodiode Amplifiers--Op Amp Solutions.* New York: McGraw-Hill, 1995.

[15] M. Johnson, *Photodetection and Measurement*. New York: McGraw-Hill, 2003.